

Late Oligocene climate and floristic diversity of Assam, Northeast India

HARSHITA BHATIA^{1,2}, GAURAV SRIVASTAVA^{1,2*} AND R.C. MEHROTRA¹

¹Birbal Sahni Institute of Palaeosciences, 53 University Road, Lucknow 226 007, India.

²Academy of Scientific and Innovative Research (AcSIR), Ghaziabad 201 002, India.

*Corresponding author: gaurav_jan10@yahoo.co.in

(Received 29 December, 2020; revised version accepted 12 July, 2021)

ABSTRACT

Bhatia H, Srivastava G & Mehrotra RC 2020. Late Oligocene climate and floristic diversity of Assam, Northeast India. The Palaeobotanist 69(1–2): 73–92.

Late Oligocene is considered as the last significant globally warm climate. In India, the Makum Coalfield has exposures of sediments which were deposited at a low latitude of 10–15° N during the late Oligocene. Here, we report a diverse assemblage of fossil leaves and fruits. The assemblage envelops 18 leaf and 9 fruit morphotypes. The floristic assemblage indicates a warm and humid climate during the deposition of the sediments. The quantitative palaeoclimate reconstruction indicates that the leaf morphological traits were dominantly adapted to Indonesian–Australian type of monsoon.

Key-words—Fossils, CLAMP, Monsoon, Oligocene, Palaeoclimate.

असम, पूर्वोत्तर भारत की विलंबित जलवायु एवं पादपी विविधता

हर्षिता भाटिया, गौरव श्रीवास्तव एवं आर.सी. मेहरोत्रा

सारांश

विलंबित अल्पनूतन अंतिम महत्वपूर्ण भू-मंडलीय रूप से कोष्ण जलवायु के रूप में माना जाता है। भारत में, मकुम कोयलाक्षेत्र अवसादों का अनावरण है जो विलंबित अल्पनूतन के दौरान 10–15° उत्तर के अल्प अक्षांश पर निक्षेपित हो गए थे। यहां हम जीवाश्म पत्तियों एवं फलों की एक भिन्न समुच्चय वर्णित करते हैं। समुच्चय 18 पत्ती व 9 फल चित्ररूप आवृत्त करती है। पादप समुच्चय अवसादों के निक्षेपण के दौरान कोष्ण एवं आर्द्र जलवायु द्योतित करती है। मात्रात्मक पुराजलवायु पुनर्चना इंगित करती है कि पत्ती आकारिकीय लक्षण प्रबलता से मानसून के इंडोनेशियाई–आस्ट्रेलियाई प्रकार से अनुकूलित हो गए थे।

सूचक शब्द—जीवाश्म, क्लैम्प, मानसून, अल्पनूतन, पुराजलवायु।

INTRODUCTION

THE late Oligocene (Chattian 28.4–23 Ma) is an important period during the Cenozoic because it represents the last episode of pronounced globally warmth climate (Zachos *et al.*, 2001). In India, the best exposure for late Oligocene sediments is present in the Makum Coalfield of northeast India. After the collision of the Indian Plate with the Eurasian Plate, northeast India acted as a corridor for the migration of biota from India to Southeast Asia and vice-versa (Srivastava & Mehrotra, 2010b; Chatterjee *et al.*, 2013). The Makum

Coalfield (27°15'–27°25'N; 95°40'–95°55'E) which is located in Assam, archived an extremely rich floristic diversity and a wide variety of vegetation types, however, evergreen forests dominated a larger part of the vegetation (Awasthi *et al.*, 1992; Awasthi & Mehrotra, 1995; Mehrotra *et al.*, 2009; Srivastava & Mehrotra, 2010a, 2012, 2013a–d; Srivastava *et al.*, 2012a). Infact, there is no other Oligocene sedimentary basin in India containing such a rich and diversified assemblage of plants.

The sediments of the Makum Coalfield were deposited at 10°–15° N palaeolatitude (Molnar & Stock, 2009) in a deltaic, mangrove or lagoonal environment (Awasthi & Mehrotra,

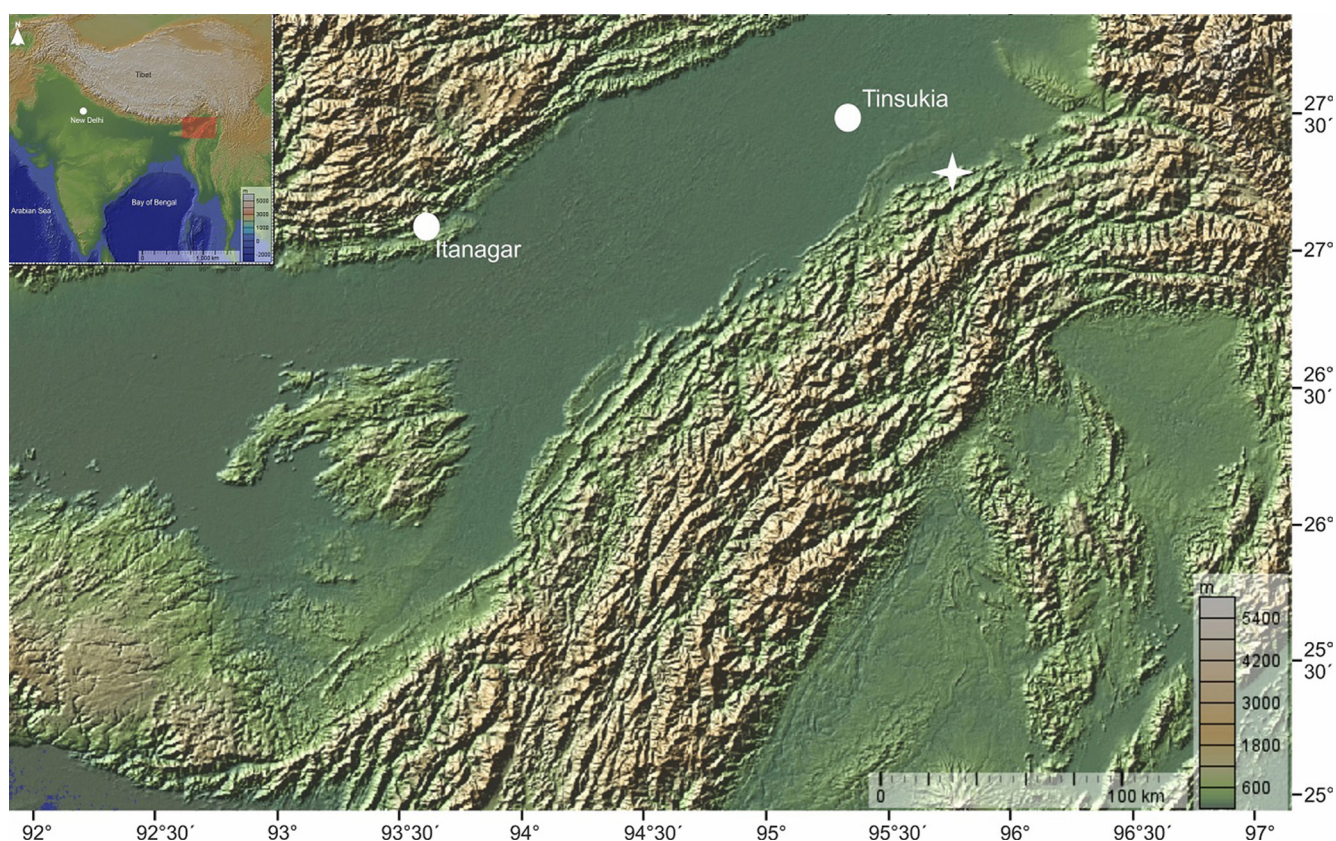


Fig. 1—A physiographic map showing the fossil locality (white asterisk).

1995; Mehrotra *et al.*, 2003; Srivastava *et al.*, 2012b). The Makum Coalfield which is the largest coalfield of northeast India, is situated in the Tinsukia District of Assam (Fig. 1) and comprises six collieries, namely Baragolai, Ledo, Namdang, Tikak, Tipong and Tirap. The Tikak Parbat Formation measures 300–600 m in thickness depending on location and encloses alternations of sandstone, siltstone, mudstone, shale, carbonaceous shale, clay and coal seams (Kumar *et al.*, 2012). It is underlain by 300 m thick predominantly sandstones that comprise the Baragolai Formation which in turn is underlain by 1100–1700 m thick Noagaon Formation (Mishra & Ghosh, 1996). Together the three formations comprise the Barail Group (Fig. 2). Numerous plant megafossils have been excavated and reported from the Tikak Parbat Formation which is considered to be late Oligocene in age on the basis of regional lithostratigraphy (Pascoe, 1964), remote sensing (Ganju *et al.*, 1986) and palynostratigraphy (Kumar *et al.*, 2012). The plant assemblage belongs to the families Anacardiaceae, Annonaceae, Arecaceae, Apocynaceae, Avicenniaceae, Burseraceae, Calophyllaceae, Clusiaceae, Combretaceae, Equisetaceae, Euphorbiaceae, Fabaceae, Lauraceae, Lecythydaceae, Malvaceae, Meliaceae, Memecylaceae, Myristicaceae, Phyllanthaceae, Poaceae, Podocarpaceae, Rhizophoraceae, and Sapindaceae (Table 1). Based on the floristic assemblage (Table 1) it can be

inferred that it contains taxa mainly belonging to tropical wet evergreen to moist deciduous and littoral and swampy forest types (Fig. 3).

In the present communication, we describe 27 different morphotypes of leaves (18) and fruits (9) unearthed from the Tirap Mine of Makum Coalfield, Assam.

MATERIAL AND METHODS

The material used for the present study was collected from the Tirap Mine (27°17'20" N; 95°46'15" E) of Makum Coalfield (Fig. 1). The dust present over the fossils was removed using a soft brush and clearing of the sediments was done with the help of a chisel and hammer. The photographs were taken under low angled sunlight using 10-megapixel digital camera (Canon SX110). Dilcher (1974) and Ellis *et al.* (2009) have been followed for describing the fossils. All the studied fossil specimens are deposited in the Museum of the Birbal Sahni Institute of Palaeosciences, Lucknow.

SYSTEMATICS

ANGIOSPERMS

DICOTYLEDONAE

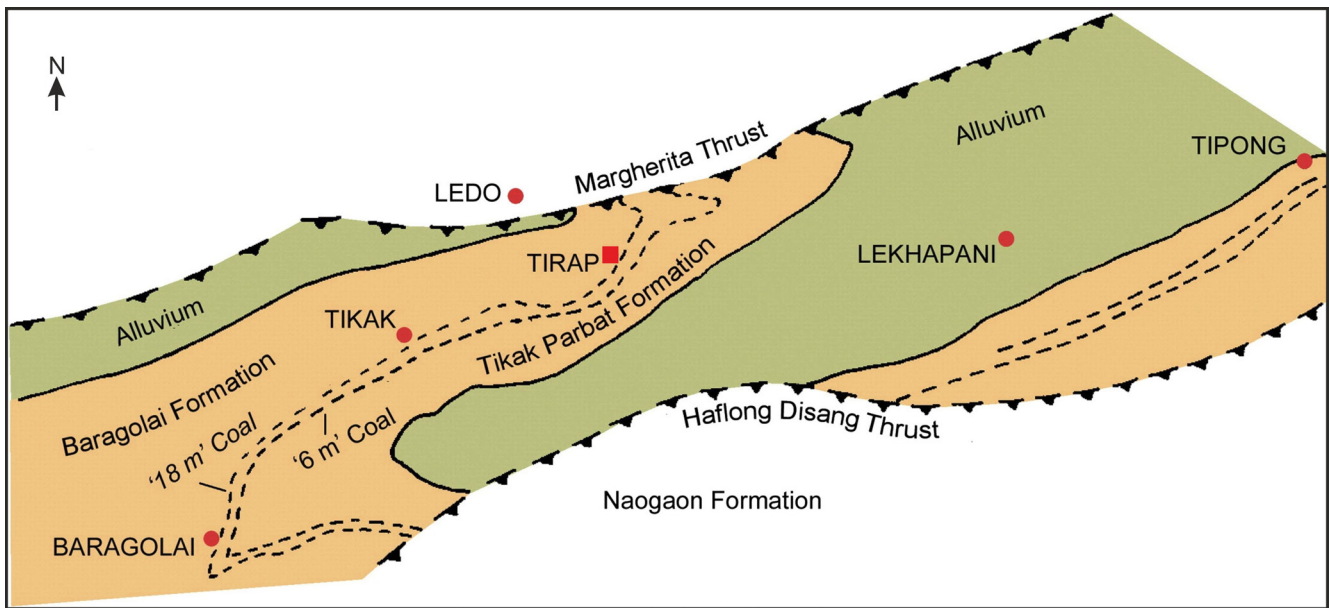


Fig. 2—Simplified geological map of the Makum Coalfield, Assam (after Ahmed, 1996).

Leaf morphotype 1

(Pl. 1.1)

Description—Leaf symmetrical, elliptic with medial symmetry, preserved lamina length 7.5 cm, maximum preserved width 5.1 cm, unlobed, entire margin; apex angle acute with seemingly attenuate shape; base not preserved; primary venation pinnate; secondary veins 7–8 pairs visible, eucamptodromous, distance between secondary veins varies 0.6–1.3 cm, angle of divergence ranging from moderate to wide acute (55°–73°) with decurrent to slightly excurrent attachment to the midvein; intersecondary veins present, covering > 50% length of the subjacent secondary veins, frequency >1, ranging 1–2 per intercoastal area, proximal course parallel to secondary, distal course terminating at percurrent tertiary; intercoastal tertiary veins percurrent, straight to slightly wavy, predominantly opposite sometimes alternate, dominantly RR–RA angle of origin; areoles poorly preserved.

Figured specimen—Specimen No. BSIP 41947.

Remarks—The above characters show that the fossil belongs to a dicot leaf. In the absence of a leaf base and other fine details it is difficult to assign it up to the family and genus level.

Leaf morphotype 2

(Pl. 1.2)

Description—Leaf symmetrical, oblong with medial symmetry, preserved lamina length 4.5 cm, maximum width

1.9 cm; lamina unlobed with entire margin; apex angle acute; base broken with seemingly acute angle; primary venation pinnate with evident striations; major secondaries, intersecondaries and tertiaries poorly preserved.

Figured specimen—Specimen No. BSIP 41948.

Discussion—Based on the characters described, the fossil can be assigned as a dicot leaf. The absence of base, faintly preserved veins and other details make it difficult to assign it to any family and genus.

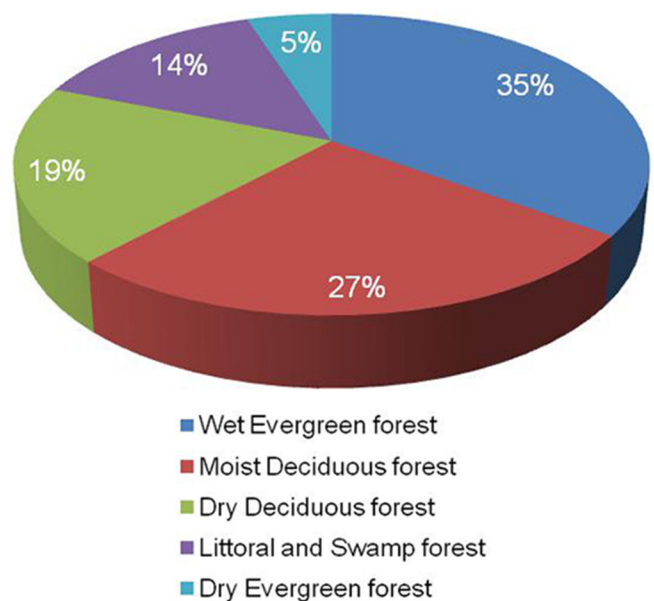


Fig. 3—Pie diagram showing different forest types present during the late Oligocene in the Makum Coalfield, Assam, India.

Table 1—List of the modern comparable taxa of the fossils reported from the Makum Coalfield, Assam.

Fossil species	Modern NLRs	References
Anacardiaceae		
<i>Lannea oligocenica</i> Awasthi & Mehrotra	<i>Lannea coromandelica</i>	Awasthi & Mehrotra (1995)
<i>Mangifera someshwarica</i> Lakhnupal & Awasthi	<i>Mangifera indica</i>	Awasthi & Mehrotra (1995)
<i>Parishia palaeoinsignis</i> Awasthi & Mehrotra	<i>Parishia insignis</i>	Awasthi & Mehrotra (1995)
<i>Semecarpus oligocenicus</i> Srivastava & Mehrotra	<i>Semecarpus anacardium</i>	Srivastava & Mehrotra (2012)
Annonaceae		
<i>Alphonsea makumensis</i> Srivastava & Mehrotra	<i>Alphonsea</i>	Srivastava & Mehrotra (2013a)
<i>Saccopetalum palaeolongiflorum</i> Awasthi & Mehrotra	<i>Saccopetalum longiflorum</i>	Awasthi & Mehrotra (1995)
Apocynaceae		
<i>Alistonia oligocenica</i> Awasthi & Mehrotra	<i>Alistonia</i>	Awasthi & Mehrotra (1995)
Areaceae		
<i>Nypa</i> Steck	<i>Nypa fruticans</i>	Mehrotra <i>et al.</i> (2003)
<i>Iguanura wallichiana</i> (Mart.) Becc.	<i>Iguanura wallichiana</i>	Srivastava & Mehrotra (2012a)
<i>Palmacites makumensis</i> Srivastava <i>et al.</i>	Areaceae	Srivastava & Mehrotra (2012a)
Avicenniaceae		
<i>Avicennia obovata</i> Awasthi & Mehrotra	<i>Avicennia officinalis</i>	Awasthi & Mehrotra (1995)
Burseraceae		
<i>Santiria oligocenica</i> Awasthi & Mehrotra	<i>Santiria laevigata</i>	Awasthi & Mehrotra (1995)
Calophyllaceae		
<i>Calophyllum suraikholaensis</i> Awasthi & Prasad	<i>Calophyllum polyanthum</i>	Awasthi & Mehrotra (1995)
Clusiaceae		
<i>Garcinia palaeoluzoniensis</i> Awasthi & Mehrotra	<i>Garcinia</i>	Awasthi & Mehrotra (1995)
<i>Kayea baragolaensis</i> Awasthi & Mehrotra	<i>Kayea floribunda</i>	Awasthi & Mehrotra (1995)
<i>Mesua antiqua</i> Awasthi <i>et al.</i>	<i>Mesua ferrea</i>	Awasthi <i>et al.</i> (1992)
<i>M. antiqua</i> Awasthi <i>et al.</i>	<i>Mesua</i>	Mehrotra <i>et al.</i> (2009)
<i>Poeciloneuron preindicum</i> Srivastava & Mehrotra	<i>Poeciloneuron indicum</i>	Srivastava & Mehrotra (2013b)
Combretaceae		
<i>Terminalia palaeocatappa</i> Awasthi & Mehrotra	<i>Terminalia catappa</i>	Awasthi & Mehrotra (1995)
<i>T. palaeochebula</i> Awasthi & Mehrotra	<i>T. chebula</i>	Awasthi & Mehrotra (1995)
<i>T. panandhroensis</i> Lakhnupal & Guleria	<i>T. coriacea</i>	Awasthi & Mehrotra (1995)
<i>T. obovata</i> Awasthi & Mehrotra	<i>T. crenulata</i>	Awasthi & Mehrotra (1995)
Equisetaceae	<i>Equisetum</i>	Mehrotra <i>et al.</i> (2009)
<i>Equisetum</i> sp.		
Fabaceae		
<i>Buteocarpum awasthii</i> Srivastava & Mehrotra	<i>Butea</i>	Srivastava & Mehrotra (2010a)
<i>B. oligocenicum</i> Srivastava & Mehrotra	<i>B. frondosa</i>	Srivastava & Mehrotra (2010a)
<i>Leguminocarpon barailensis</i> Srivastava & Mehrotra	Fabaceae	Srivastava & Mehrotra (2010a)
<i>L. makumensis</i> Srivastava & Mehrotra	Fabaceae	Srivastava & Mehrotra (2010a)

<i>L. lakhampalii</i> Srivastava & Mehrotra	Fabaceae	Srivastava & Mehrotra (2010a)
<i>L. tirapensis</i> Srivastava & Mehrotra	Fabaceae	Srivastava & Mehrotra (2010a)
<i>L. dilcheri</i> Srivastava & Mehrotra	Fabaceae	Srivastava & Mehrotra (2010a)
<i>L. baragolaiensis</i> Srivastava & Mehrotra	Fabaceae	Srivastava & Mehrotra (2010a)
<i>L. dalbergioides</i> Awasthi & Mehrotra	<i>Dalbergia sissoo</i>	Awasthi & Mehrotra (1995)
<i>Leguminocarpon</i> Goepfert	Fabaceae	Srivastava & Mehrotra (2010a)
<i>Entada palaeoscandens</i> Awasthi & Prasad	<i>Entada phaseoloides</i>	Awasthi & Mehrotra (1995)
Lauraceae		
<i>Apollonias litseoides</i> Awasthi & Mehrotra	<i>Apollonias arnottii</i>	Awasthi & Mehrotra (1995)
<i>Daphnogene makumensis</i> Mehrotra <i>et al.</i>	Lauraceae	Mehrotra <i>et al.</i> (2009)
Lecythidaceae		
<i>Barringtonia preraacemosa</i> Mehrotra	<i>Barringtonia racemosa</i>	Mehrotra (2000)
<i>Careyoxylon kuchilense</i> Prakash & Tripathi	<i>Careya</i>	Mehrotra & Srivastava (2017)
<i>Barringtonia</i> Forster & Forster	<i>Barringtonia</i>	Srivastava & Mehrotra (2018)
Malvaceae		
<i>Pterygota cordata</i> Awasthi & Mehrotra	<i>Pterygota alata</i>	Awasthi & Mehrotra (1995)
<i>Sterculia palaeovillosa</i> Mehrotra	<i>Sterculia</i>	Mehrotra (2000)
<i>Firmiana oligocenica</i> Srivastava & Mehrotra	<i>Firmiana colorata</i>	Srivastava & Mehrotra (2013c)
<i>Pterygota palaeoalata</i> Srivastava & Mehrotra	<i>Pterygota alata</i>	Srivastava & Mehrotra (2013c)
Meliaceae		
<i>Heynea trijugoides</i> Awasthi & Mehrotra	<i>Heynea trijuga</i>	Awasthi & Mehrotra (1995)
Memecylaceae		
<i>Memecylon amplexicaulensis</i> Awasthi & Mehrotra	<i>Memecylon amplexicaule</i>	Awasthi & Mehrotra (1995)
Myristicaceae		
<i>Myristica lorata</i> Awasthi & Mehrotra	<i>Myristica sylvestris</i>	Awasthi & Mehrotra (1995)
Phyllanthaceae		
<i>Bridelia oligocenica</i> Awasthi & Mehrotra	<i>Bridelia retusa</i>	Awasthi & Mehrotra (1995)
<i>Bridelia makumensis</i> Srivastava & Mehrotra	<i>Bridelia</i>	Srivastava & Mehrotra (2014)
Podocarpaceae		
<i>Podocarpus oligocenicus</i> Awasthi <i>et al.</i>	<i>Podocarpus nerifolius</i>	Awasthi <i>et al.</i> (1992)
Poaceae		
<i>Bambusiculmus makumensis</i> Srivastava & Mehrotra	Bambusoideae	Srivastava <i>et al.</i> (2019)
<i>Bambusiculmus tirapensis</i> Srivastava & Mehrotra	Bambusoideae	Srivastava <i>et al.</i> (2019)
Rhizophoraceae		
<i>Rhizophora coriacea</i> Awasthi & Mehrotra	<i>Rhizophora mucronulata</i>	Awasthi & Mehrotra (1995)
Sapindaceae		
<i>Nephelium oligocenicum</i> Awasthi & Mehrotra	<i>Nephelium longama</i> & <i>N. rubescens</i>	Awasthi & Mehrotra (1995)
<i>Paranephelium makumensis</i> Srivastava & Mehrotra	<i>Paranephelium xestophyllum</i>	Srivastava & Mehrotra (2013c)
<i>Sapindus palaeoemarginatus</i> Srivastava & Mehrotra	<i>Sapindus emarginatus</i>	Srivastava & Mehrotra (2013c)

Leaf morphotype 3

(Pl. 1.3)

Description—Leaf slightly asymmetrical, elliptic with medial symmetry, preserved lamina length 2.85 cm, maximum width 1.75 cm; lamina unlobed with entire margin; apex missing; base asymmetrical, angle obtuse with convex shape; primary venation pinnate; major secondaries 5–6 pairs visible, festooned brochidodromous, with excurrent attachment to the midvein; intersecondaries present, covering < 50% length of the subjacent secondaries, proximal course perpendicular to midvein, distal course of intersecondaries reticulate or ramified, frequency >1, ranging 1–2 per intercoastal area; intercoastal tertiary veins irregular reticulate, forming irregular nets; quaternary veins present; polygonal shaped areoles with variable size.

Figured specimen—Specimen No. BSIP 41949.

Remarks—Present fossil leaf shows the characters of a dicotyledonous leaf.

Leaf morphotype 4

(Pl. 1.4)

Description—Leaf incomplete, elliptic with medial asymmetry, preserved lamina length 3.1 cm, maximum width 3.5 cm; lamina unlobed with entire margin; apex broken; base asymmetrical with acute angle and convex shape; primary venation pinnate; long petiole present; major secondaries 2–3 pairs visible, eucamptodromous venation with irregular spacing ranging from 0.53–0.65 cm with excurrent attachment to the midvein; intersecondaries and tertiaries not clearly visible.

Figured specimen—Specimen No. BSIP 41950.

Remarks—Characters described above show that the fossil is a dicot leaf. Systematic assignment of the fossil is difficult due to poorly preserved apex and venation details.

Leaf morphotype 5

(Pl. 2.1)

Description—Leaf symmetrical, elliptic with medial symmetry, preserved lamina length 5 cm, maximum width 3.4 cm; lamina unlobed with entire margin; apex missing; base asymmetrical with obtuse angle and convex shape; primary venation pinnate; long petiole present; major secondaries 6 pairs visible, brochidodromous with irregular spacing ranging from 0.41–0.88 cm, angle of divergence ranging from narrow to wide acute (37°–66°) with decurrent attachment to the midvein; intersecondaries present, covering > 50% length of the subjacent secondaries, proximal course perpendicular to midvein, distal course of intersecondary parallel to secondaries terminating into percurrent tertiaries, frequency >1, ranging 1–2 per intercoastal area; intercoastal tertiary veins percurrent, straight to slightly wavy, predominantly opposite, sometimes alternate, dominantly RR–RA angle of origin; epimedial tertiaries absent; exterior tertiaries looped; areoles polygonal in shape, size variable.

Figured specimen—Specimen No. BSIP 41951.

Remarks—The above characters indicate that the fossil is a dicot leaf. Due to broken apex, it is difficult to assign the fossil to its systematic position.

Leaf morphotype 6


(Pl. 2.2)

Description—Leaf symmetrical, elliptic with medial symmetry, preserved lamina length 4.7 cm, maximum width 3.2 cm; lamina unlobed with entire margin; apex missing; base angle obtuse, convex shape with a swollen petiole; primary venation pinnate; texture coriaceous; major secondaries 3–4 pairs visible, eucamptodromous with irregular spacing ranging from 0.52–0.69 cm, angle of divergence ranging from moderate to wide acute (53°–67°) with excurrent attachment to the midvein; intersecondaries not distinctly visible; intercoastal tertiary veins percurrent, straight to slightly wavy, predominantly opposite to sometimes alternate; areoles poorly preserved.

Figured specimen—Specimen No. BSIP 41952.

Remarks—Present fossil leaf shows the characters of a dicotyledonous leaf.

PLATE 1

Different morphotypes of fossil dicot leaves showing shape, size and venation pattern (All bar scales = 1 cm). 

1. Leaf morphotype 1 showing elliptic shape, medial symmetry, pinnate venation of midvein (white arrows), eucamptodromous venation of secondary veins (yellow arrows), intersecondaries veins (black arrows) with percurrent intercoastal tertiaries (pink arrow). Specimen No. BSIP 41947.
2. Leaf morphotype 2 showing symmetrical leaf with oblong shape and pinnate midvein (black arrows). Specimen No. BSIP 41948.
3. Leaf morphotype 3 showing asymmetrical lamina and base, pinnate midvein (white arrow), festooned brochidodromous (yellow arrows) venation of secondaries, intersecondaries veins (black arrows) and reticulate intercoastal tertiary veins (green arrows). Specimen No. BSIP 41949.
4. Leaf morphotype 4 showing asymmetrical base, pinnate midvein (white arrow), a long petiole and eucamptodromous venation of secondaries (yellow arrows). Specimen No. BSIP 41950.



PLATE 1

Leaf morphotype 7

(Pl. 2.3)

Description—Leaf incomplete, symmetrical, elliptic with medial symmetry, preserved lamina length 4.9 cm, maximum width 4.3 cm, unlobed with entire margin; apex missing; base angle acute; primary venation pinnate; secondary veins one pair visible, arising from basal part of lamina and running parallel to the margin; intersecondary veins not visible; intercoastal tertiary vein percurrent, predominantly opposite sometimes alternate, dominantly RR–RA angle of origin, exmedial tertiary veins looped; areoles poorly preserved.

Figured specimen—Specimen No. BSIP 41953.

Remarks—Present fossil leaf shows the characters of a dicotyledonous leaf, however, due to poor preservation of the fossil it is difficult to assign it at the family and genus level.

Leaf morphotype 8

(Pl. 2.4)

Description—Leaf complete, symmetrical, elliptic with medial symmetry, lamina length 3.18 cm, width 1.66 cm; lamina unlobed with entire margin; apex angle obtuse with round shape; base angle acute with decurrent shape; primary venation pinnate; major secondaries, intersecondaries, tertiary and other details not discernible.

Figured specimen—Specimen No. BSIP 41954.

Remarks—Due to ill preserved venation pattern, it is difficult to assign the fossil to its systematic position.

Leaf morphotype 9

(Pl. 3.1)

Description—Leaf incomplete, appearing symmetrical, elliptic with medial symmetry, preserved lamina length 13 cm, maximum width 9.5 cm; lamina unlobed with entire margin; apex missing; base missing, seemingly convex, primary venation pinnate; major secondaries 5–6 pairs visible, eucamptodromous with irregular spacing ranging from 1.1–3

cm, angle of divergence ranging from moderate to wide acute (64° – 80°) with excurrent attachment to the midvein, course straight to slightly curved upward joining with adjacent secondaries at the margin; intersecondaries present, covering < 50% length of the subjacent secondaries, frequency >1, ranging 1–2 per intercoastal area. Intercoastal tertiary veins percurrent, straight to slightly wavy, predominantly opposite to sometimes alternate, dominantly RR–RO angle of origin; epimedial tertiaries opposite percurrent; exterior tertiaries looped; areoles poorly preserved, shape and size variable.

Figured specimen—Specimen No. BSIP 41955.

Remarks—Characters described above show that the fossil is a dicot leaf. Fragmentary nature of leaf hinders its correct determination and assignment to a systematic position.

Leaf morphotype 10

(Pl. 3.2)

Description—Leaf appearing symmetrical, elliptic with medial symmetry, preserved lamina length 6.6 cm, maximum width 3.7 cm; lamina unlobed with entire margin; apex broken; base broken; primary venation pinnate. Major secondaries 8–9 pairs visible, eucamptodromous with irregular spacing ranging from 0.40–0.60 cm, angle ranging from moderate to wide acute (62° – 74°) with excurrent attachment to the midvein; intersecondaries present, with frequency >1, ranging 1–2 per intercoastal area; intercoastal tertiary veins faintly preserved; areoles poorly preserved.

Figured specimen—Specimen No. BSIP 41956.

Remarks—Based on the characters described above, the fossil can be assigned to a dicot leaf. Due to broken apex, faintly preserved tertiaries and other details it is difficult to assign the fossil to its family and natural genus.

Leaf morphotype 11

(Pl. 3.3)

Description—Leaf slightly asymmetrical, elliptic with medial symmetry, preserved lamina length 1.85 cm,

PLATE 2

Different morphotypes of fossil dicot leaves showing shape, size and venation pattern (All bar scales = 1 cm).



1. Leaf morphotype 5 showing symmetrical, elliptic leaf with pinnate midvein (white arrow), asymmetrical base with a long petiole, brochidodromous secondaries (yellow arrows) having decurrent attachment with midvein, intersecondaries covering > 50% length of the subjacent secondary veins (black arrows), intercoastal tertiary (pink arrows) veins percurrent, straight to slightly wavy, predominantly opposite sometimes alternate. Specimen No. BSIP 41951.
2. Leaf morphotype 6 showing pinnate midvein (white arrow), obtuse base angle, secondaries (yellow arrows) and percurrent intercoastal tertiaries (pink arrow). Specimen No. BSIP 41952.
3. Leaf morphotype 7 showing midvein (white arrow), with secondaries arising from the basal part of lamina and running parallel along the margin (yellow arrows) and looped exmedial tertiaries (green arrows). Specimen No. BSIP 41953.
4. Leaf morphotype 8 showing round apex, pinnate midvein (white arrows) and decurrent base. Specimen No. BSIP 41954.

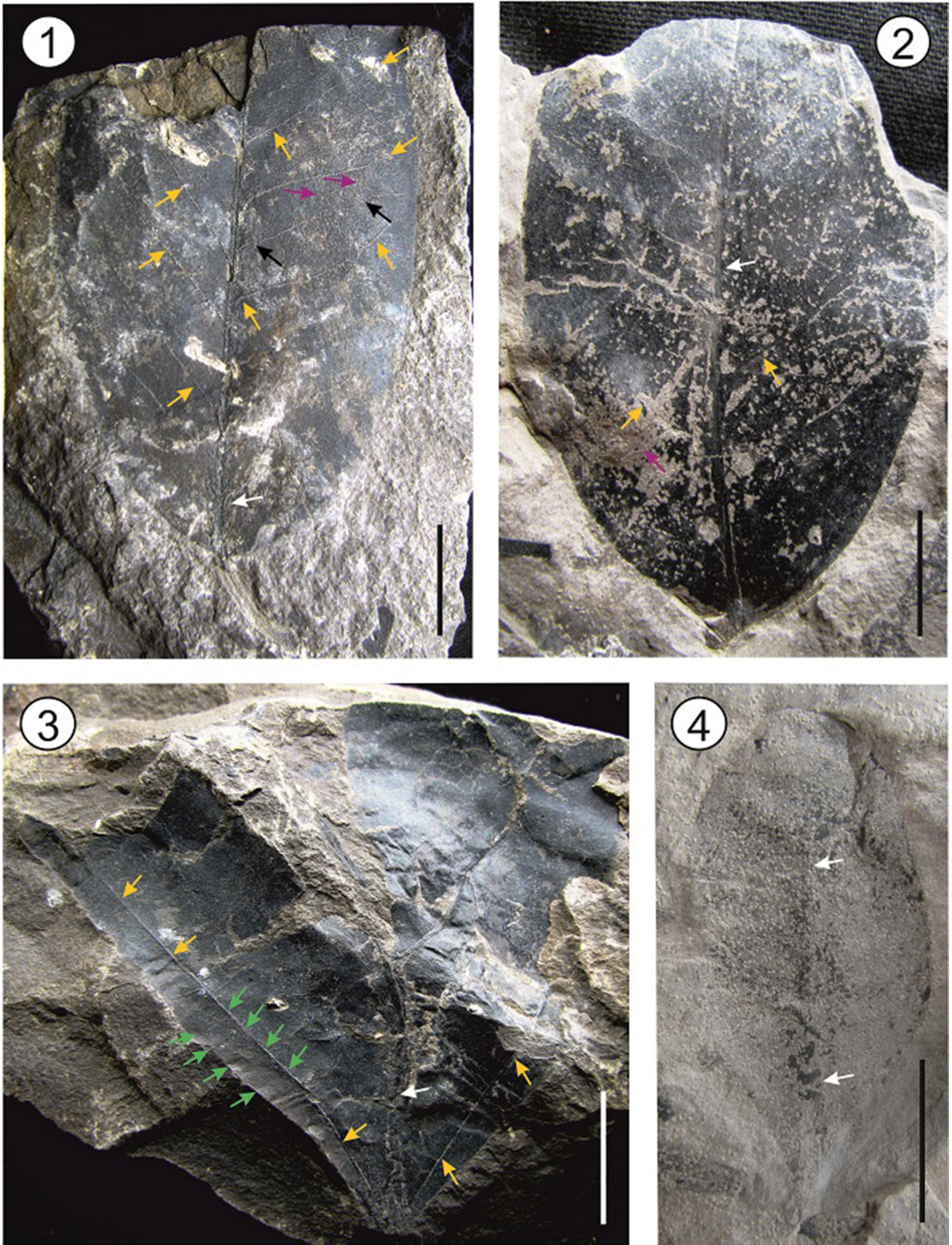


PLATE 2

maximum width 0.95 cm; lamina unlobed with entire margin; apex broken; base angle acute with convex shape; primary venation pinnate; major secondaries 4–5 pairs visible, eucamptodromous venation with irregular spacing ranging from 0.19–0.27 cm, angle of divergence ranging from moderate acute to right angle (50° – 87°) with excurrent attachment to the midvein; intersecondaries and tertiary veins faintly preserved; areoles not visible.

Figured specimen—Specimen No. BSIP 41957.

Remarks—The above characters show that the fossil is a dicot leaf. Due to incomplete preservation of veins and other details it is difficult to assign the fossil to its family.

Leaf morphotype 12

(Pl. 3.4)

Description—Leaf appearing symmetrical, elliptic with medial symmetry, preserved lamina length 6.5 cm, maximum width 2.9 cm; lamina unlobed with entire and wavy margin; apex broken; base angle seemingly acute; primary venation pinnate; striations observed on the midvein; major secondaries 4 pairs visible, eucamptodromous venation with irregular spacing ranging from 0.67–1.21 cm, angle of divergence ranging from moderate to wide acute (65° – 75°) with excurrent to slightly decurrent attachment to the midvein; intersecondaries present, covering < 50% length of the subjacent secondary, frequency >1, ranging 1–2 per intercoastal area; intercoastal tertiary veins percurrent, straight to slightly wavy, predominantly opposite, angle of origin dominantly AO; epimedial tertiaries opposite percurrent; exterior tertiary seemingly looped; areoles poorly preserved.

Figured specimen—Specimen No. BSIP 41958.

Remarks—Characters described above show that the fossil is a dicot leaf. Fragmentary nature of the leaf hinders its correct determination and assignment to a systematic position.

Leaf morphotype 13

(Pl. 3.5)

Description—Leaf incomplete appearing symmetrical, elliptic with medial symmetry, preserved lamina length 6.7 cm, maximum width 4.7 cm; lamina unlobed with entire margin; apex broken; base angle acute with cuneate/straight shape, slightly asymmetrical; long and thick petiole present; primary venation pinnate; major secondaries eucamptodromous with irregular spacing ranging from 0.70–0.96 cm, angle of divergence ranging from moderate to wide acute (63° – 75°) with excurrent attachment to the midvein; intersecondary and tertiary veins faintly preserved.

Figured specimen—Specimen No. BSIP 41959.

Remarks—The above characters place the fossil into a dicot leaf. Due to the absence of apex, intersecondary veins, tertiary veins and other details it is difficult to assign the fossil to its family.

Leaf morphotype 14

(Pl. 4.1)

Description—Leaf incomplete appearing symmetrical, elliptic with medial symmetry, preserved lamina length 9.9 cm, maximum width 3.60 cm; lamina unlobed with entire margin; apex broken; base broken; primary venation pinnate; major secondaries 4–5 pairs visible, eucamptodromous with irregular spacing ranging from 1.30–2.08 cm, angle of divergence ranging from moderate to wide acute (51° – 65°) with excurrent attachment to the midvein; intersecondaries present with frequency >1, ranging 1–2 per intercoastal area; intercoastal tertiary veins percurrent, straight to slightly wavy, predominantly opposite sometimes alternate, dominantly AA–AO angle of origin; exterior tertiary looped.

Figured specimen—Specimen No. BSIP 41960.

Discussion—Based on the characters described above, the fossil can be assigned to a dicotyledonous leaf. Fragmentary nature of the leaf hinders its correct determination and assignment to a systematic position.

Leaf morphotype 15

(Pl. 4.2)

PLATE 3

Different morphotypes of fossil dicot leaves showing shape, size and venation pattern (All bar scales = 1 cm).



1. Leaf morphotype 9 showing elliptic shape, pinnate midvein (white arrow), secondaries eucamptodromous (pink arrows) with excurrent attachment to midvein, percurrent intercoastal tertiaries (yellow arrows), opposite percurrent epimedial tertiaries (blue arrows) and looped exterior tertiaries (black arrows). Specimen No. BSIP 41955.
2. Leaf morphotype 10 showing elliptic shape with pinnate midvein (white arrows), eucamptodromous secondaries (yellow arrows) with excurrent attachment to the midvein and intersecondary veins (blue arrows). Specimen No. BSIP 41956.
3. Leaf morphotype 11 showing slightly asymmetrical leaf with elliptic shape, base angle acute with convex shape, pinnate midvein (white arrow) with eucamptodromous secondaries (yellow arrow). Specimen No. BSIP 41957.
4. Leaf morphotype 12 showing elliptic shape, pinnate primary venation (white arrow), eucamptodromous secondaries (yellow arrows), percurrent intercoastal tertiary (blue arrow) and opposite percurrent epimedial tertiaries (black arrow). Specimen No. BSIP 41958.
5. Leaf morphotype 13 showing symmetrical cuneate leaf with pinnate midvein (white arrows) with eucamptodromous secondaries (yellow arrows). Specimen No. BSIP 41959.



PLATE 3

Description—Leaf incomplete, elliptic with medial symmetry, preserved lamina length 3.6 cm, maximum width 1.3 cm; lamina unlobed with entire and wavy margin; apex broken; base angle acute with seemingly convex shape; primary venation pinnate; major secondaries eucamptodromous with excurrent attachment to the midvein; intersecondaries and tertiaries not clearly visible.

Figured specimen—Specimen No. BSIP 41961.

Remarks—Based on the characters described above, the fossil can be assigned to a dicot leaf. Due to incomplete preservation of veins and other details it is difficult to assign the fossil to its systematic position.

Leaf morphotype 16

(Pl. 4.3)

Description—Leaf symmetrical, elliptic with medial symmetry, preserved lamina length 9.7 cm, maximum width 3.4 cm; lamina unlobed with entire margin; apex broken, angle seemingly acute; base broken; primary venation pinnate; major secondaries 10–11 pairs visible, eucamptodromous with irregular spacing ranging from 0.64–0.89 cm, angle of divergence ranging from moderate to wide acute (55° – 73°) with slightly decurrent to excurrent attachment to the midvein, course of secondaries straight to slightly curved upward to the margin; intersecondaries present, covering < 50% length of the subjacent secondaries, proximal course perpendicular to midvein, distal course of intersecondary parallel to secondaries terminating into percurrent tertiaries, frequency >1, ranging 2–4 per intercoastal area; intercoastal tertiary veins percurrent, straight to slightly wavy, predominantly opposite sometimes alternate, dominantly RR–RO angle of origin; exterior tertiary looped; areoles poorly preserved, shape and size variable.

Figured specimen—Specimen No. BSIP 41962.

Remarks—The above characters indicate that the fossil is a dicot leaf. In the absence of apex, base and other details it is difficult to assign the fossil to its family and natural genus.

Leaf morphotype 17

(Pl. 4.4)

Description—Leaf incomplete, elliptic in shape, preserved lamina length 9.9 cm, maximum width 6.95 cm; lamina unlobed with entire margin; apex broken; base broken; primary venation pinnate; major secondaries 2 pairs visible, eucamptodromous venation with irregular spacing ranging from 1.77–2.28 cm, angle of divergence ranging from moderate to wide acute (51° – 67°), with decurrent attachment to the midvein; intersecondaries not clearly visible; intercoastal tertiary veins faintly preserved, seemingly opposite percurrent, straight to slightly wavy, angle of origin dominantly RR–RA.

Figured specimen—Specimen No. BSIP 41963.

Remarks—The fragmentary nature of the leaf precludes a precise determination, but the general leaf shape and venation pattern assign it to a dicot leaf.

Leaf morphotype 18


(Pl. 4.5)

Description—Leaf appearing symmetrical, elliptic with medial symmetry, preserved lamina length 9.1 cm, maximum width 7.7 cm; lamina unlobed with entire margin; apex missing; base angle obtuse with convex shape; primary venation pinnate with evident striations; major secondaries 4 pairs visible, eucamptodromous venation with irregular spacing ranging from 0.83–2.55 cm, angle ranging from moderate to wide acute (47° – 80°) with slightly decurrent to excurrent attachment to the midvein; intersecondaries present, covering < 50% length of the subjacent secondaries, frequency >1, ranging 1–2 per intercoastal area; intercoastal tertiary veins percurrent, straight to slightly wavy, predominantly opposite, angle of origin AO–RO; epimedial tertiaries opposite percurrent, exterior tertiary veins seemingly looped; areoles poorly preserved.

Figured specimen—Specimen No. BSIP 41964.

Remarks—Present fossil leaf shows the characters of a dicotyledonous leaf. Due to fragmentary nature of the leaf it is difficult to assign it to the family level. Insect damage on the fossil leaf is clearly visible. At some places insect mine is also present.

PLATE 4

Different morphotypes of fossil dicot leaves showing shape, size and venation pattern (All bar scales = 1 cm). 

1. Leaf morphotype 14 showing pinnate midvein (white arrows), eucamptodromous secondary veins (yellow arrows) and intersecondary veins (blue arrow). Specimen No. BSIP 41960.
2. Leaf morphotype 15 showing elliptic leaf with pinnate midvein (white arrow), acute base, eucamptodromous secondaries (yellow arrows) with excurrent attachment to the midvein. Specimen No. BSIP 41961.
3. Leaf morphotype 16 showing elliptic shape, medial symmetry, pinnate midvein (white arrows), eucamptodromous secondaries (yellow arrows), intersecondary veins (blue arrows) with percurrent tertiaries (pink arrow). Specimen No. BSIP 41962.
4. Leaf morphotype 17 showing elliptic leaf with pinnate midvein (white arrow), eucamptodromous secondaries (black arrows) and percurrent intercoastal tertiary veins (yellow arrow). Specimen No. BSIP 41963.
5. Leaf morphotype 18 showing elliptic shape with pinnate midvein (white arrows), eucamptodromous secondaries (yellow arrows), intersecondary veins (black arrow), intercoastal tertiary veins percurrent (pink arrows) and epimedial tertiary veins opposite percurrent (blue arrows). Specimen No. BSIP 41964.

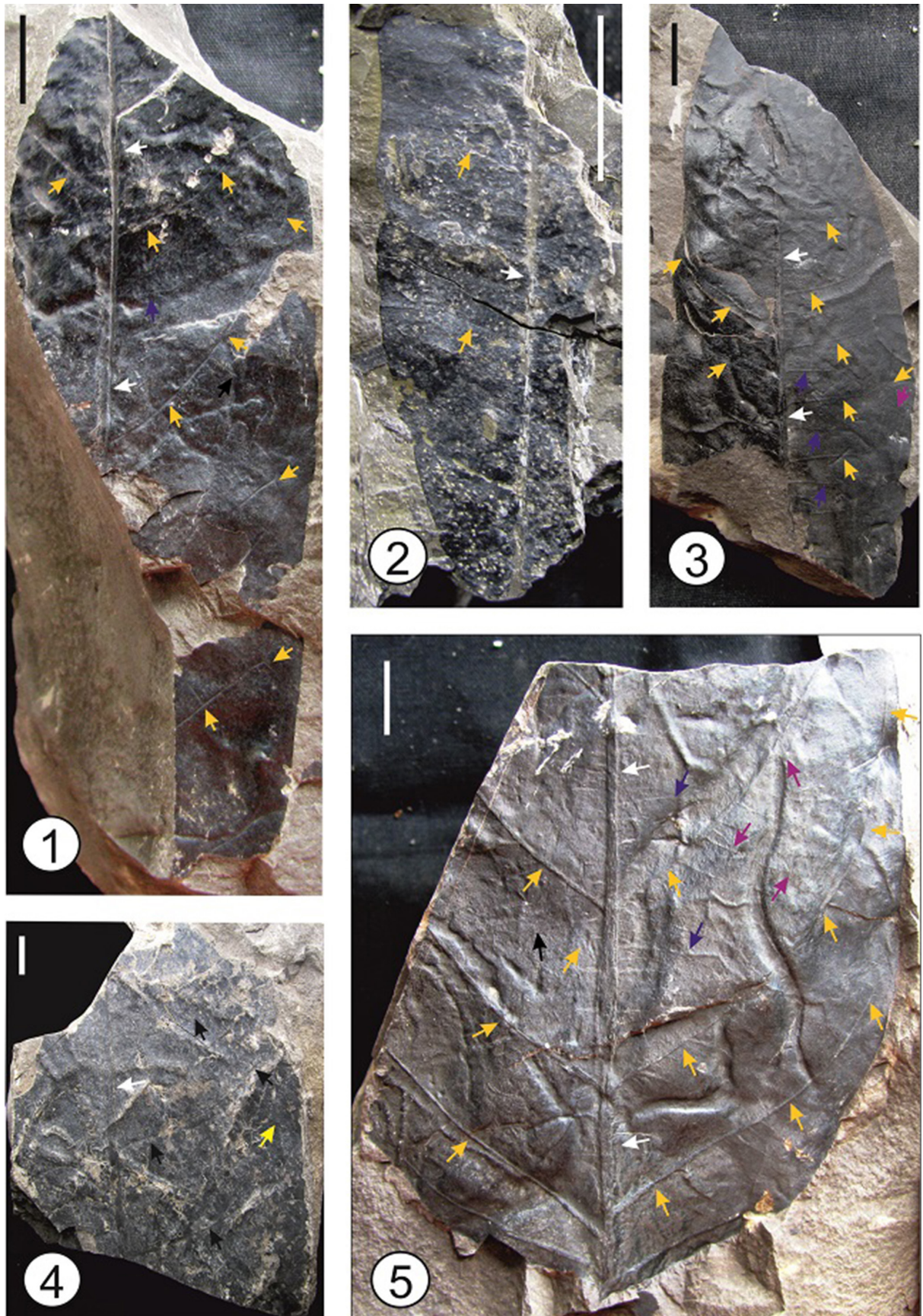


PLATE 4

Fruit morphotype 1

(Pl. 5.1)

Description—Fruit ovate; length 5.3 cm; width 2.1 cm; apex angle acute with presence of a long beak, length 1.4 cm and width 0.49 cm; base angle obtuse with slightly rounded appearance; striations present on the surface, closely spaced, running parallel to the margin, but coalescing at the apex and base.

Figured specimen—Specimen No. BSIP 41965.

Remarks— Fossil fruit with similar appearance has been described by Mehrotra *et al.* (2009) from the Makum Coalfield, but it was different in size, shape and length of the beak from the present fossil. Due to lack of many peculiar features, it is difficult to compare the fossil with the modern analogue.

Fruit morphotype 2

(Pl. 5.2)

Description—Fruit elliptic or slightly oblong in appearance; preserved length 2.9 cm, width 1.1 cm; apex slightly broken with acute angle; base obtuse with slightly rounded appearance; striations present on the surface, closely spaced, running parallel to the margin, but converging apically and basally.

Figured specimen—Specimen No. BSIP 41966.

Remarks—Due to lack of apical features and other marginal characters comparison of the fossil with the modern taxa is difficult.

Fruit morphotype 3

(Pl. 5.3)

Description—Fruit ovate; preserved length 2.8 cm, width 1.80 cm; apex angle acute, tip of the apex slightly broken; base angle obtuse with round shape; striations present all over the surface, closely spaced, running parallel to the margin, but coalescing at the apex and base.

Figured specimen—Specimen No. BSIP 41967.

Remarks—Absence of many peculiar features makes it difficult to assign it to its systematic position.

Fruit morphotype 4

(Pl. 5.4)

Description—Fruit round or slightly elliptic in appearance; preserved length 3.3 cm, width 2.4 cm; apex angle obtuse, terminally broken; beak slightly preserved; base angle obtuse with slightly rounded appearance; striations present on the surface, closely spaced, running parallel to the margin, but coalescing apically and basally.

Figured specimen—Specimen No. BSIP 41968.

Remarks—Due to its broken beak and other details the fossil precludes a precise determination and comparison with living genus.

Fruit morphotype 5

(Pl. 5.5)

Description—Fruit elliptic, swollen in middle; length 3.8 cm; width 1.95 cm; apex angle acute; short beak present having round terminal end, beak length 0.59 cm and width 0.27 cm; base slightly broken with obtuse angle; striations present on the surface, not closely spaced, running parallel to the margin.

Figured specimen—Specimen No. BSIP 41969.

Remarks—Due to its common shape and size, it is difficult to ascertain its affinity with modern analogues. The

PLATE 5

Different morphotypes of fossil fruits showing shape, size and other characteristic features (All bar scales = 1 cm).



1. Fruit morphotype 1 showing ovate fruit with a long beak (black arrows) and striations on the surface (yellow arrows). Specimen No. BSIP 41965.
2. Fruit morphotype 2 showing elliptic fruit, apex angle acute and obtuse base angle with striations on the surface (yellow arrows). Specimen No. BSIP 41966.
3. Fruit morphotype 3 showing ovate fruit, acute apex angle, obtuse base angle with round shape and striations (yellow arrow) on the surface running parallel to the margin but coalescing at the apex and base. Specimen No. BSIP 41967.
4. Fruit morphotype 4 showing round or slightly elliptic fruit, slightly preserved beak (black arrow) round base with striations (yellow arrows) on the surface running parallel to the margin but coalescing at the apex and base. Specimen No. BSIP 41968.
5. Fruit morphotype 5 showing elliptic fruit with a short beak (black arrows) and obtuse base angle with striations (yellow arrows) on the surface. Specimen No. BSIP 41969.
6. Fruit morphotype 6 showing elliptic fruit, obtuse base angle with convex shape and striations (yellow arrow) on the surface closely spaced and running parallel to the margin. Specimen No. BSIP 41970.
7. Fruit morphotype 7 showing ovate fruit, apex angle acute, obtuse base angle with round shape and striations (yellow arrow) on the surface. Specimen No. BSIP 41971.
8. Fruit morphotype 8 showing elliptic fruit with a smooth suture (yellow arrows). Specimen No. BSIP 41972.
9. Fruit morphotype 9 showing seemingly round fruit with striations (yellow arrows) on the surface running parallel to the margin but coalescing at the apex and base. Specimen No. BSIP 41973.

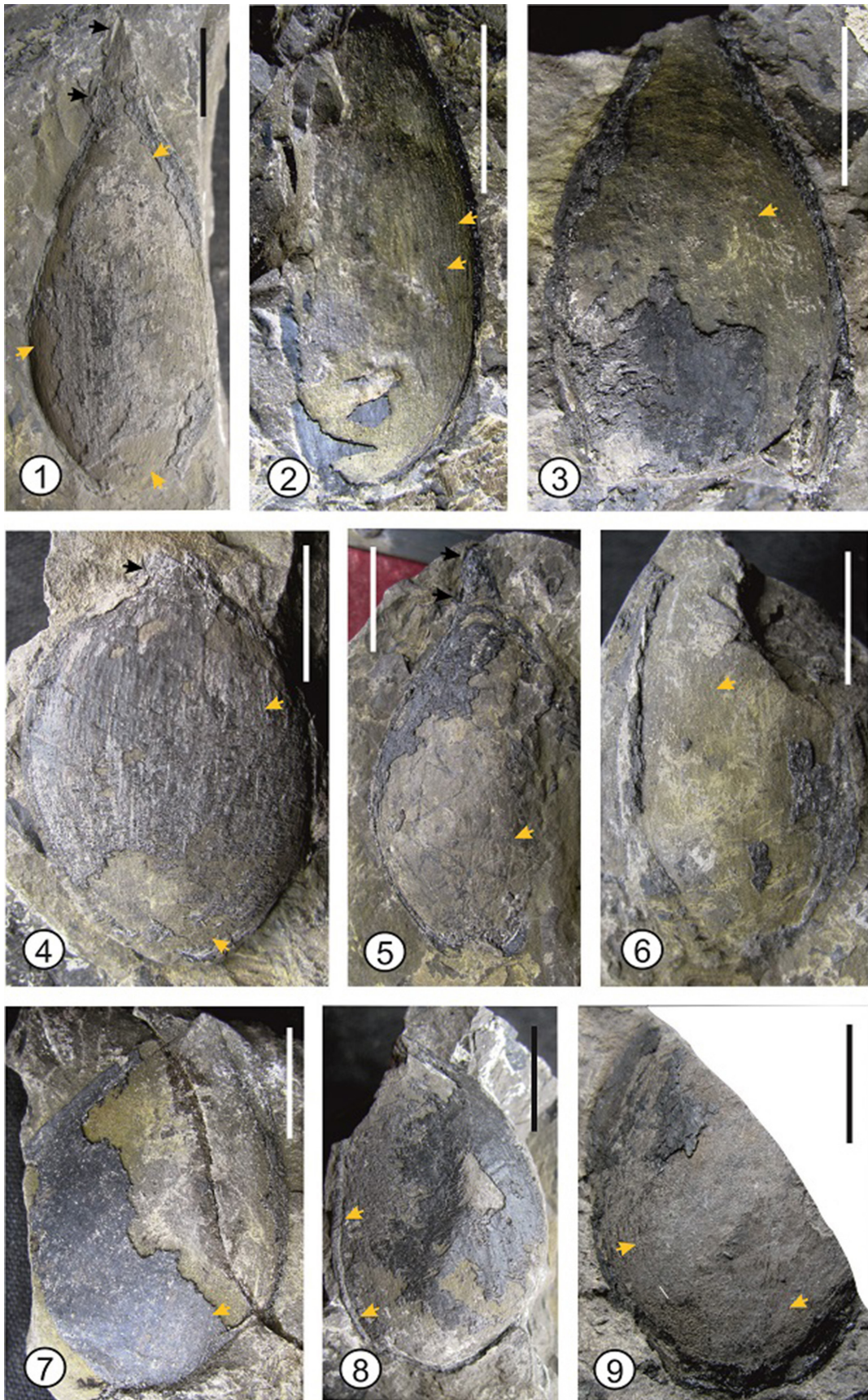


PLATE 5

present fossil can be differentiated from the fossil described by Mehrotra *et al.* (2009) in having elliptic shape and size.

Fruit morphotype 6

(Pl. 5.6)

Description—Fruit elliptic in appearance; preserved length 3.4 cm, width 1.5 cm; apex angle acute, slightly broken; base angle obtuse with convex shape; striations present on the surface, closely spaced, running parallel to the margin, but converging apically and basally.

Figured specimen—Specimen No. BSIP 41970.

Remarks—The fossil fruit is very common in appearance and difficult to be identified with any extant genus.

Fruit morphotype 7

(Pl. 5.7)

Description—Fruit ovate or slightly round in appearance; length 3.3 cm; width 2.1 cm; apex angle acute, terminally broken; base angle obtuse with round shape; striations slightly visible.

Figured specimen—Specimen No. BSIP 41971.

Remarks—In the absence of many peculiar details it is difficult to compare it with modern taxa. The absence of prominent striations and size difference make it apart from the fossil described by Mehrotra *et al.* (2009).

Fruit morphotype 8

(Pl. 5.8)

Description—Fruit elliptic; preserved length 3.30 cm, width 2.04 cm; apex angle appearing acute; base angle obtuse, convex in shape; smooth suture present; closely spaced striations running parallel to the margin.

Figured specimen—Specimen No. BSIP 41972.

Remarks—The presence of suture makes it distinct from rest of the fossil fruits described above. Due to incomplete preservation and other details it is difficult to assign it correct systematic position.

Fruit morphotype 9

(Pl. 5.9)

Description—Fruit incomplete, seemingly round or elliptic in appearance; preserved length 3.4 cm, width 2.2 cm; apex missing; base angle obtuse with slightly rounded appearance; striations present on the surface, closely spaced, running parallel to the margin, but coalescing apically and basally.

Figured specimen—Specimen No. BSIP 41973.

Remarks—Due to its broken apex and other details it precludes a precise determination and comparison with living genus.

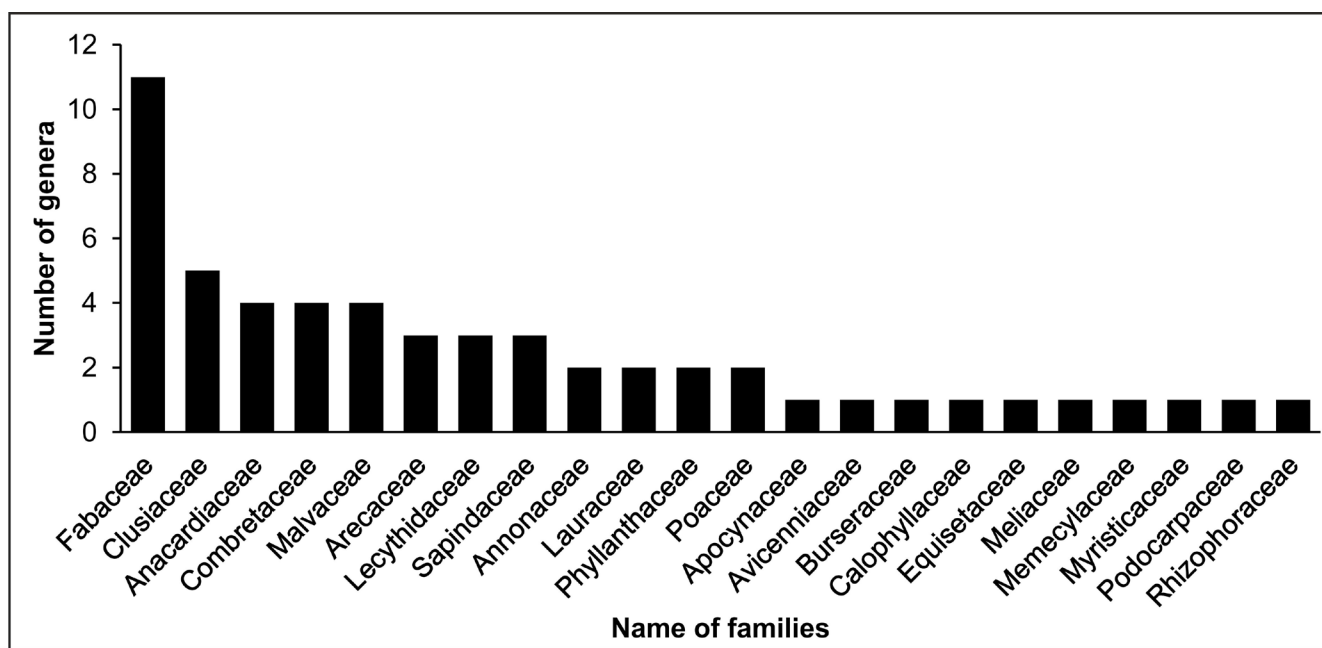


Fig. 4—Floristic bar diagram showing the diversity and dominance of various families present in the Makum coalfield during the late Oligocene in Assam.

DISCUSSION

The Makum Coalfield is important because of the highly diversified and rich plant fossil assemblage. In fact, there is no other comparable late Oligocene sedimentary basin in India sustaining such high diversity of plant fossils. The Makum Coalfield archived plant fossil assemblage in the form of leaves, fruits, wood and seeds which were preserved at low latitude during the time when the earth was globally warm (Zachos *et al.*, 2001).

The climate of late Oligocene of the Makum Coalfield has been reconstructed by qualitative as well as quantitative studies. The qualitative reconstructed climate data based on the floristic assemblage (Table 1) (Fig. 4) indicates the dominance of moist evergreen taxa. Moreover, families such as Annonaceae, Burseraceae, Clusiaceae, Combretaceae, Lecythidaceae, Myristicaceae and Rhizophoraceae have pantropical distribution (van Steenis, 1962) and their presence suggests that the CMMT (Cold Month Mean Temperature) was not less than 18°C (Srivastava *et al.*, 2012b). The dominance of Fabaceae (Srivastava & Mehrotra, 2010a) also indicates a distinct seasonality in rainfall with warm climate (Punyasena *et al.*, 2008). The occurrence of Avicenniaceae and Rhizophoraceae is highly indicative of deltaic and mangrove type of vegetation in the Makum Coalfield. Moreover, the presence of palms like *Nypa* provides evidence of a coastal plain environment where both temperature and humidity remained high throughout the year (Tomlinson, 1990). The overall floristic assemblage of Makum Coalfield indicates the dominance of tropical and wet conditions (Fig. 3).

The quantitative estimation of palaeoclimate of the Makum Coalfield has been done by CLAMP (climate leaf analysis multivariate program) analysis (Srivastava *et al.*, 2012b). The CLAMP analysis is based on the relationship between leaf morphological traits and their prevailing climatic conditions (Wolfe, 1993; Yang *et al.*, 2015).

Srivastava *et al.* (2012b) have used 80 different leaf morphotypes for CLAMP analysis. The leaves were numerically scored strictly following the CLAMP protocol given on its webpage (http://clamp.ibcas.ac.cn/CLAMP_Home.html). Out of 31 leaf physiognomic characters used in the CLAMP, two are the most dominant, i.e. entire margin (score 100%) and elliptic shape (97.5%) which suggest high temperature and rainfall (Wolfe, 1993). The CLAMP analysis on the Tirap Mine fossil flora indicates a MAT (Mean Annual Temperature) of $26.09 \pm 2.7^\circ\text{C}$, WMMT (Warm Month Mean Temperature) of $27.85 \pm 3.3^\circ\text{C}$, CMMT (Cold Month Mean Temperature) of $20.66 \pm 4.3^\circ\text{C}$, MAP (Mean Annual Precipitation) of 2460 ± 614 mm and RH (Relative Humidity) of $76.6 \pm 12.6\%$. The reconstructed temperature data indicates that the seasonality in the WMMT and CMMT was less pronounced. The warm and humid climate of the fossil locality

is not surprising as it was at 10° – 15° N palaeolatitude, i.e. near the equator during the late Oligocene (Molnar & Stock, 2009). The precipitation estimates suggest a marked seasonality in the rainfall pattern showing a wet season with 20 times the rainfall of the dry season. The high ratio of WET: DRY season indicates a monsoonal type of climate during the deposition of the sediments (Srivastava *et al.*, 2012b).

Generally, the monsoon can be defined as the annual reversal of surface wind often associated with wet summer and dry winter seasons (Wang *et al.*, 2017). Globally monsoons have been categorized into North America Monsoon (NAMM), South America Monsoon (SAMM), North Africa Monsoon (NAfM), South Africa Monsoon (SAfM), Asian Monsoon (AM) and Indonesian–Australian Monsoon (I–AM). The monsoonal climate is a manifestation of the movement of the Intertropical Convergence Zone (ITCZ). The movement of ITCZ depends on the seasonal distribution of solar insolation and rainfall intensity depends on the atmospheric energy balance (Schneider *et al.*, 2014). The different domains and characteristic features of the global monsoon depend on the land–sea distribution and topography of the region (Wang *et al.*, 2017). The AM is further sub–divided into South Asia Monsoon (SAM), East Asia Monsoon (EAM) and Western North Pacific Monsoon (WNPM) (Wang *et al.*, 2017).

The evolution of AM dates back to Late Cretaceous and Paleogene (Ghosh *et al.*, 1995; Srivastava *et al.*, 2012b; Licht *et al.*, 2014; Shukla *et al.*, 2014; Spicer *et al.*, 2016, 2017; Liu *et al.*, 2017; Ghosh *et al.*, 2018; Farnsworth *et al.*, 2019). The leaf morphological traits are economically tuned to adapt in all the seasons to perform maximum photosynthesis with minimum transpirational loss (Givnish, 1984). This adaptation of leaf physiognomy to its prevailing climatic condition characterizes it to adapt in the monsoonal and non–monsoonal climate (Spicer *et al.*, 2017; Bhatia *et al.*, 2021). The fossil leaf physiognomy of Tirap Mine of the Makum Coalfield, Assam in the global physiognomic space indicates that it is more adapted to the I–AM type of monsoon, along with some adaption to the SAM (Fig. 5). This suggests that the characteristic SAM was most likely established after the late Oligocene. The recent studies indicate that the characteristic SAM is topographically driven monsoon and is mainly governed by the Himalaya (Molnar *et al.*, 2010; Boos & Kuang, 2010; Ding *et al.*, 2017; Bhatia *et al.*, 2021).

Acknowledgements—*The authors are thankful to the authorities of the Coal India Limited (Northeastern Region), Margherita for permission to collect plant fossils from the Makum Coalfield and to Dr Vandana Prasad, Director, Birbal Sahni Institute of Palaeosciences, Lucknow for providing necessary facilities and permission to carry out the present work. The authors are thankful to anonymous reviewers for their valuable suggestions in improving the manuscript.*

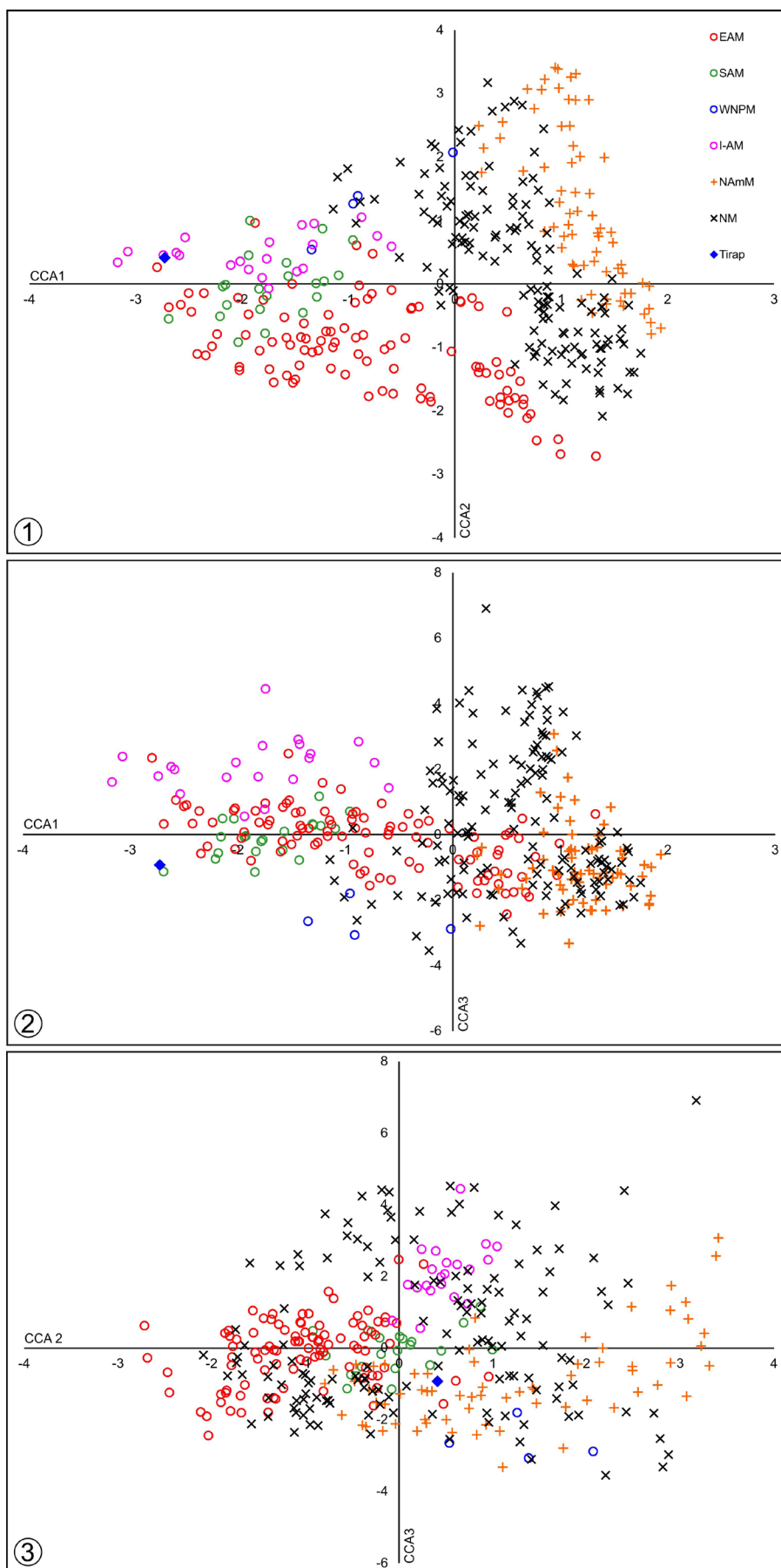


Fig. 5—CCA plots showing the distribution and adaptation of fossil and modern leaves according to their prevailing monsoonal and non-monsoonal climate in the physiognomic space. The symbols represented are EAM—East Asia Monsoon, SAM—South Asia Monsoon, WNPM—Western North Pacific Monsoon, I—AM—Indonesian—Australian Monsoon, NAmM—North American Monsoon, NM—No Monsoon and solid diamond (blue color)—Tirap Mine (modified after Spicer *et al.*, 2017).

REFERENCES

- Ahmed M 1996. Petrology of Oligocene coal, Makum Coalfield, Assam, northeast India. *International Journal of Coal Geology* 30: 319–325.
- Awasthi N & Mehrotra RC 1995. Oligocene flora from Makum Coalfield, Assam, India. *Palaeobotanist* 44: 157–188.
- Awasthi N, Mehrotra RC & Lakhanpal RN 1992. Occurrence of *Podocarpus* and *Mesua* in the Oligocene sediments of Makum Coalfield, Assam, India. *Geophytology* 22: 193–198.
- Bhatia H, Srivastava G, Spicer RA, Farnsworth A, Spicer TEV, Mehrotra RC, Paudyal K & Valdes PJ 2021. Leaf physiognomy records the Miocene intensification of the South Asian Monsoon. *Global & Planetary Change* 196: <https://doi.org/10.1016/j.gloplacha.2020.103365>, 103365.
- Boos WR & Kuang Z 2010. Dominant control of the South Asian monsoon by Orographic insulation versus plateau heating. *Nature* 463: 218–222.
- Chatterjee S, Goswami A & Scotese CR 2013. The longest voyage: Tectonic, magmatic and paleoclimatic evolution of the Indian Plate during its northward flight from Gondwana to Asia. *Gondwana Research* 23: 238–267.
- Dilcher DL 1974. Approaches to the identification of angiosperm leaf remains. *Botanical Review* 40: 1–157.
- Ding L, Spicer RA, Yang J, Xu Q, Ca F, Li S, Lai Q, Wang H, Spicer TEV, Yue Y, Shukla A, Srivastava G, Khan MA, Bera S & Mehrotra R 2017. Quantifying the rise of the Himalaya orogen and implications for the South Asian monsoon. *Geology* 45: 215–218.
- Ellis B, Daly D, Hickey LJ, Johnson KR, Mitchell J, Wilf P & Wing SL 2009. *Manual of leaf architecture*. Cornell University Press, Ithaca, New York.
- Farnsworth A, Lunt DJ, Robinson SA, Valdes PJ, Roberts WHG, Clift PD, Markwick P, Tao S, Wrobel N, Bragg F, Kelland S–J & Pancost RD. 2019. Past east Asian monsoon evolution controlled by palaeogeography, not CO₂. *Science Advances* 5: eaax 1697.
- Ganju JI, Khare BM & Chaturvedi JS 1986. Geology and hydrocarbon prospect of Naga Hills south of 27° latitude. *Bulletin of Oil and Natural Gas Commission* 23: 129–145.
- Ghosh P, Bhattacharya SK & Jani RA 1995. Palaeoclimate and palaeovegetation in central India during the Upper Cretaceous based on stable isotope composition of the palaeosol carbonates. *Palaeogeography, Palaeoclimatology, Palaeoecology* 114: 285–296.
- Ghosh P, Prasanna K, Banerjee Y, Williams IS, Gagan MK, Chaudhuri A & Suwas S 2018. Rainfall seasonality on the Indian subcontinent during the Cretaceous greenhouse. *Scientific Reports* 8: 8482.
- Givnish TJ 1984. Leaf and canopy adaptations in tropical forest. *In: Medina E, Mooney HA & Vázquez-Yanes C (Editors) —Physiological ecology of plants of the wet tropics: 51–84*. Junk, The Hague.
- Kumar M, Srivastava G, Spicer RA, Spicer TEV, Mehrotra RC & Mehrotra NC 2012. Sedimentology, palynostratigraphy and palynofacies of the late Oligocene Makum Coalfield, Assam, India: a window on lowland tropical vegetation during the most recent episode of significant global warmth. *Palaeogeography, Palaeoclimatology, Palaeoecology* 342–343: 143–162.
- Licht A, van Cappelle M, Abels HA, Ladant JB, Trabuco–Alexandre J, France–Lanord C, Donnadiu Y, Vandenberghé J, Rigaudier T, Lecuyer C, Terry D, Adriaens R, Boura A, Guo Z, Soe AN, Quade J, Dupont–Nivet G & Jaeger JJ 2014. Asian monsoons in a Late Eocene greenhouse world. *Nature* 513: 501–506.
- Liu X, Dong B, Yin Z–Y, Smith RS & Guo Q 2017. Continental drift and plateau uplift control origination and evolution of Asian and Australian monsoon. *Scientific Reports* 7: 40344.
- Mehrotra RC 2000. Two new fossil fruits from Oligocene sediments of Makum Coalfield, Assam, India. *Current Science* 79: 1482–1483.
- Mehrotra RC, Dilcher DL & Lott TA 2009. Notes on elements of the Oligocene flora from the Makum Coalfield, Assam, India. *Palaeobotanist* 58: 1–9.
- Mehrotra RC, Tiwari RP & Mazumder BI 2003. *Nypa* megafossils from the Tertiary sediments of northeast India. *Geobios* 36: 83–92.
- Mishra HK & Ghosh RK 1996. Geology, petrology and utilization of some Tertiary coals of the northeastern region of India. *International Journal of Coal Geology* 30: 65–100.
- Molnar P & Stock JM 2009. Slowing of India's convergence with Eurasia since 20 Ma and its implications for Tibetan mantle dynamics. *Tectonics* 28: TC3001.
- Molnar P, Boos WR & Battisti DS 2010. Orographic controls on climate and paleoclimate of Asia: thermal and mechanical roles for the Tibetan Plateau. *Annual Review of Earth and Planetary Sciences* 38: 77–102.
- Pascoe EH 1964. *A manual of the geology of India and Burma*. Geological Survey of India, Calcutta.
- Punyasena SW, Eshel G & McElwain JC 2008. The influence of climate on the spatial patterning of neotropical plant families. *Journal of Biogeography* 35: 117–130.
- Schneider T, Bischoff T & Haug GH 2014. Migrations and dynamics of the intertropical convergence zone. *Nature* 513: 45–53.
- Shukla A, Mehrotra RC, Spicer RA, Spicer TEV & Kumar M 2014. Cool equatorial terrestrial temperatures and the South Asian monsoon in the Early Eocene: evidence from the Gurha Mine, Rajasthan, India. *Palaeogeography, Palaeoclimatology, Palaeoecology* 412: 187–198.
- Spicer RA, Yang J, Herman AB, Kodrul T, Maslova N, Spicer TEV, Aleksandrova G & Jin J–J 2016. Asian Eocene Monsoons as revealed by leaf architectural signatures. *Earth and Planetary Science Letters* 449: 61–68.
- Spicer RA, Yang J, Herman AB, Kodrul T, Aleksandrova G, Maslova N, Spicer TEV, Ding L, Xu Q, Shukla A, Srivastava G, Mehrotra R, Liu X–Y & Jin J–J 2017. Paleogene monsoons across India and South China: drivers of biotic change. *Gondwana Research* 49: 350–363.
- Srivastava G & Mehrotra RC 2010a. New legume fruits from the Oligocene sediments of Assam. *Journal of the Geological Society of India* 75: 820–828.
- Srivastava G & Mehrotra RC 2010b. Tertiary flora of northeast India vis-à-vis movement of the Indian Plate. *Geological Society of India Memoir* 75: 123–130.
- Srivastava G & Mehrotra RC 2012. Oldest fossil of *Semecarpus* L.f. from the Makum Coalfield, Assam, India and comments on its origin. *Current Science* 102: 398–400.
- Srivastava G & Mehrotra RC 2013a. First fossil record of *Alphonsea* Hk. f. & T. (Annonaceae) from the late Oligocene sediments of Assam, India and comments on its phytogeography. *Plos One* 8 (1): e53177.
- Srivastava G & Mehrotra RC 2013b. Endemism due to climate change: Evidence from *Poeciloneuron* Bedd. (Clusiaceae) leaf fossil from Assam, India. *Journal of Earth System Science* 122: 283–288.
- Srivastava G & Mehrotra RC 2013c. Further contribution to the low latitude leaf assemblage from the late Oligocene sediments of Assam and its phytogeographical significance. *Journal of Earth System Science* 122: 1341–1357.
- Srivastava G & Mehrotra RC 2013d. Low latitude floral assemblage from the Late Oligocene sediments of Assam and its palaeoclimatic and palaeogeographic significance. *Chinese Science Bulletin* 58: 156–161.
- Srivastava G & Mehrotra RC 2014. Phytogeographical implication of *Bridelia* Willd. (Phyllanthaceae) fossil leaf from the Late Oligocene of India. *Plos One* 9(10): e111140.
- Srivastava G & Mehrotra RC 2018. *Barringtonia* Forster & Forster (Lecythidaceae) leaf from the late Oligocene of Assam, India. *Palaeobotanist* 67: 139–145.
- Srivastava G, Mehrotra RC & Bauer H 2012a. Palm leaves from the Late Oligocene sediments of Makum Coalfield, Assam. *Journal of Earth System Science* 121: 747–754.
- Srivastava G, Spicer RA, Spicer TEV, Yang J, Kumar M, Mehrotra R & Mehrotra N 2012b. Megafloora and palaeoclimate of a Late Oligocene tropical delta, Makum Coalfield, Assam: Evidence for the early development of the South Asia Monsoon. *Palaeogeography, Palaeoclimatology, Palaeoecology* 342–343: 130–142.
- Srivastava G, Su T, Mehrotra RC, Kumari P & Shankar U 2019. Bamboo fossils from Oligo–Pliocene sediments of northeast India with implications on their evolutionary ecology and biogeography in Asia. *Review of Palaeobotany & Palynology* 262: 17–27.
- Tomlinson PB 1990. *The structural biology of palms*. Clarendon Press, Oxford.

- van Steenis CGGJ 1962. The land-bridge theory in botany. *Blumea* 11: 235–372.
- Wang PX, Wang B, Cheng H, Fasullo J, Guo Z-T, Liu Z-Y & Kiefer T 2017. The global monsoon across time scales: Mechanisms and outstanding issues. *Earth-Science Reviews* 174: 84–121.
- Wolfe JA 1993. A method of obtaining climatic parameters from leaf assemblages. *Bulletin of the United States Geological Survey* 2040: 1–73.
- Yang J, Spicer RA, Spicer TEV, Arens NC, Jacques FMB, Su T, Kennedy EM, Herman AB, Steart DC, Srivastava G, Mehrotra RC, Valdes PJ, Mehrotra NC, Zhou Z & Lai JS 2015. Leaf form–climate relationships on the global stage: an ensemble of characters. *Global Ecology and Biogeography* 24: 1113–1125.
- Zachos J, Pagani M, Sloan L, Thomas E & Billups K 2001. Trends, rhythms and aberrations in global climate 65 Ma to present. *Science* 292: 686–693.